



Content from this work may be used under the terms of the CC BY 3.0 licence (© 2019). Any distribution of this work must maintain attribution to the author(s), title of the work, publisher, and DOI

is using TRACE 3-D, which uses matrix multiplication to obtain beam characteristics for any section of the beam line [6].

The layout of the beam line, as shown in Fig. 1, has two bending magnets and four quadrupoles to assist with the optics matching.

In the matching, the proton beam of 10 MeV-50 MeV and 10  $\mu$ A was simulated respectively, and the parameters of each quadrupole were adjusted in the matching to get the size of the beam spot on the target is  $\Phi$ 20 mm.

Figure 2 shows the optics matching results for 30 MeV and 50 MeV. The protons in this energy range can be directly extracted from the cyclotron without the degrader. The matching starts from the exit of the cyclotron. Figure 2 also shows the envelope in both horizontal and vertical directions, the upper one is the optics result of 50 MeV beam and the nether on is 30 MeV. The magnetic field gradient of each quadrupole is shown in Table 1. The beam spot on the target for both 50 MeV and 30 MeV is  $\Phi$ 20 mm.

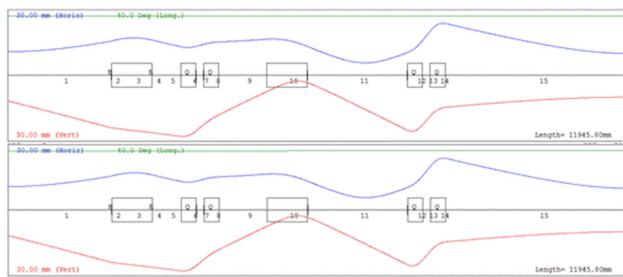


Figure 2: The optics results of 50 MeV (upper) and 30 MeV (lower).

Since the minimum energy extracted from the cyclotron is 30 MeV, the lower energy beam requires by using a degrader, the parameters of the proton beam after the degrader are determined by the collimators. In the matching, after the degrader, the beam parameter is chosen as  $x=y=8$  mm, and  $x'=y'=3$  mrad. The matching is starting at the outlet of the degrader. The optical matching results of the 20 MeV and 10 MeV proton beam are shown in Fig. 3, the upper one is the optics result of 20 MeV beam and the nether on is 10 MeV, the magnetic field gradient of each quadrupole is also shown in Table 1.

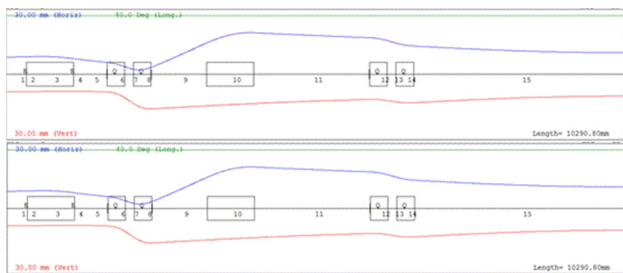


Figure 3: The optics results of 20 MeV (upper) and 10 MeV (lower).

In summary, we can adjust the parameters of each collimators and magnets to obtain the beam energy, beam spot size, envelope size and other parameters that meet the design requirements.

Table 1: Field Gradient of the Quadrupoles for Different Beam Energies

Field \ Energy	Q1 T/m	Q2 T/m	Q3 T/m	Q4 T/m
50 MeV	-2.91	1.36	-5.48	5.40
30 MeV	-2.25	1.05	-4.22	4.15
20 MeV	4.18	-2.88	0.91	-1.00
10 MeV	2.95	-2.03	0.64	-0.71

## MAGNET DESIGN

### Bending Magnet Design

There are two 45° bending magnets on the beam line, which deflects the 10 MeV~50 MeV proton beam to the terminal station and selected the beam energy. The magnetic rigidity of the 50 MeV proton is 1.034 Tm, and the bending radius of the magnet is 1 m, so the maximum magnetic field of the magnet is 1.034 T. The magnet is designed to take a maximum magnetic field of 1.1 T. According to the envelope size of the proton beam in the magnet, the field of the magnet is required to be  $\pm$ 25 mm, and the uniformity of the magnetic field is better than  $5 \times 10^{-4}$ .

The cross section of the magnet is shown in Fig. 4. This figure is a 1/4 model of the magnet cross section. To improve the uniformity of the magnetic field, the padding is added on both sides of the magnetic pole surface. Figure 4 is also shows the distribution of the magnetic field in the magnet. The magnetic field distribution in the magnet is calculated, as shown in Fig. 5. It is calculated that within  $\pm$ 25 mm of the good field, the calculated uniformity of the magnetic field is  $1.28 \times 10^{-4}$ , which satisfies the design requirements.

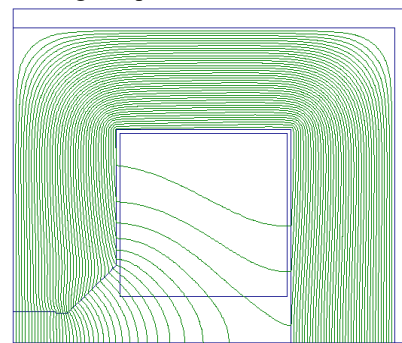


Figure 4: Cross section of the bending magnet.

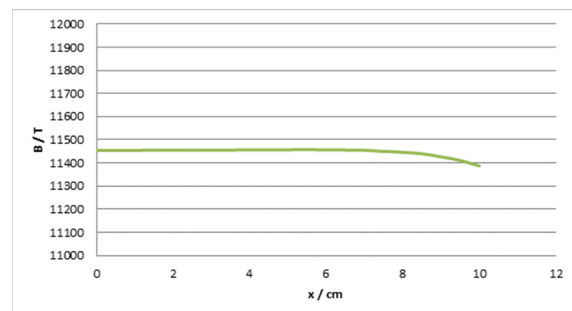


Figure 5: Field distribution along the radial center.

## Quadrupole Design

With the field gradient, the effective length, and the inner bore of the quadrupole, we can determine the pole face width and pole face shape of the magnet and the yoke thickness. Based on these basic parameters, we designed a quadrupole magnet using the two-dimensional computational magnetic field calculation program POISSON.

Based on accurate numerical analysis of magnetic fields and the past experience, here we choose a quadrupole structure with a polygonal tip section as a fold line instead of the theoretical hyperbolic structure. Such a structure has the advantages of simple processing, easy installation and positioning, etc. The difficult is to accurately designing the shape of the magnetic pole through accurate numerical analysis of the magnetic field.

Since the quadrupole magnet is an axisymmetric component, in the design we chose one-eighth model to calculate the field. The specific structure is shown in Fig. 6. The figure also shows the magnetic field of one-eighth of the magnet. distributed.

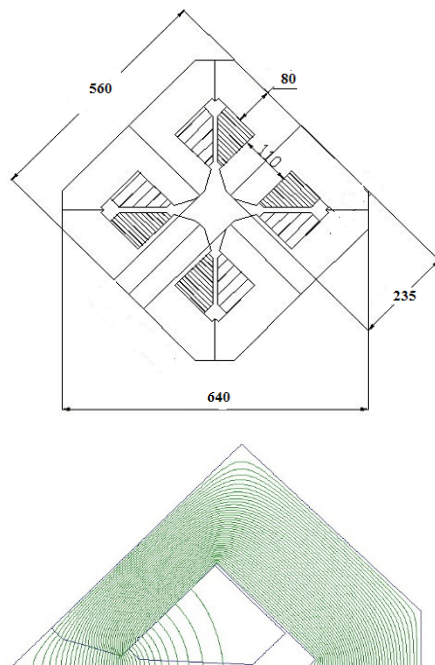


Figure 6: Cross section of the quadrupole.

## Wobbling Magnet Design

The wobbling magnet produces a periodic magnetic field perpendicular to the direction of particle motion, which produces a periodically varying force on the particle that causes the particle to scan over the target, as shown in Fig 7.

The voltage applied to the wobbling magnet changes periodically, so that the magnetic field generated by the magnet also changes periodically. The force applied to the particles changes periodically, too. The radius of the particles scanned on the target periodically changes and then get a large uniform beam spot.

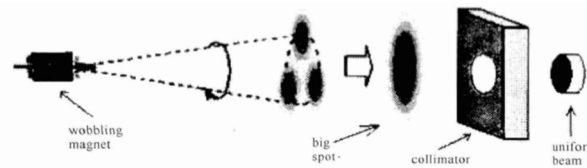


Figure 7: Working principle of the wobbling magnet.

## CONCLUSION

Based on the development of a 50 MeV compact cyclotron in the cyclotron center of CIAE, a radiation-specific proton beam line is designed to get the proton beam of 10 MeV-50 MeV, 10 nA-10  $\mu$ A.

At present, the layout design and optical matching of the beam line have been completed, and various elements such as magnets and diagnostic systems are in the process of mechanical design and processing. It is expected that the installation and beam commission will be completed in 2020.

## REFERENCES

- [1] T. Zhang *et al.*, "The cyclotron development activities at CIAE", *Nucl. Instr. Methods Phys. Res., Sect. A*, vol. 269, no. 24, pp. 2863-2870, Dec. 2011.  
doi.org/10.1016/j.nimb.2011.04.047
- [2] T. Zhang and J. Yang, "The beam commissioning of BRIF and future cyclotron development at CIAE", *Nucl. Instr. Methods Phys. Res., Sect. B*, vol. 376, pp. 434-439, Jun. 2016.  
doi.org/10.1016/j.nimb.2016.01.022
- [3] S. Wei *et al.*, "Beam line design for a 100 MeV high intensity proton cyclotron at CIAE", *Nucl. Instr. Methods Phys. Res., Sect. B*, vol. 261, no. 1-2, pp. 65-69, Aug. 2007.  
doi.org/10.1016/j.nimb.2007.04.232
- [4] S. Wei *et al.*, "Transfer beamline design after stripping", *Nucl. Instr. Methods Phys. Res., Sect. B*, vol. 266, no. 19-20, pp. 4697-4701, Oct. 2008.  
doi:10.1016/j.nimb.2008.05.119
- [5] Xianlu Jia *et al.*, "Wobbling magnet design on the beam line for a 30 MeV medical cyclotron", *High Energy Physics and Nuclear Physics*, no. 3, pp. 292-295, 2007.
- [6] K. R. Crandall and D. P. Rusthoi, *TRACE 3-D Documentation*, Third Edition, May 1997, Los Alamos National Laboratory.